ACS APPLIED MATERIALS & INTERFACES

Research Article

www.acsami.org

Photostable Bipolar Fluorescent Probe for Video Tracking Plasma Membranes Related Cellular Processes

Xinfu Zhang,[†] Chao Wang,[†] Liji Jin,[‡] Zhuo Han,[‡] and Yi Xiao*,[†]

[†]State Key Laboratory of Fine Chemicals and [‡]School of Life Science and Technology, Dalian University of Technology, Dalian 116024, China

Supporting Information

ABSTRACT: Plasma membranes can sense the stimulations and transmit the signals from extracellular environment and then make further responses through changes in locations, shapes or morphologies. Common fluorescent membrane markers are not well suited for long time tracking due to their shorter retention time inside plasma membranes and/or their lower photostability. To this end, we develop a new bipolar marker, Mem-SQAC, which can stably insert into plasma membranes of different cells and exhibits a long retention time over 30 min. Mem-SQAC also inherits excellent photostability from the BODIPY dye family. Large two-photon absorption cross sections and long wavelength fluorescence emissions further enhance the competitiveness of Mem-SQAC as a membrane marker. By using Mem-SQAC, significant morphological changes of plasma membranes have been monitored during heavy metal poisoning and drug induced apoptosis of MCF-7 cells; the change tendencies are so distinctly different from each other that they can be used as indicators to distinguish different cell injuries. Further on, the complete processes of endocytosis toward *Staphylococcus aureus* and *Escherichia coli* by RAW 264.7 cells have been dynamically tracked. It is discovered that plasma membranes take quite different actions in response to the two bacteria, information unavailable in previous research reports.

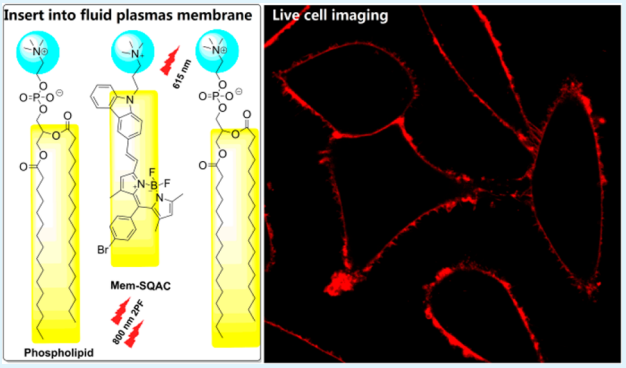

KEYWORDS: *plasma membrane, probe, long wavelength, two-photon, fluorescence imaging*

INTRODUCTION

Plasma membranes, as the channel for exchanging information and substances between cells and their surroundings, undergo continuous dynamic changes.[1−3] The capability to instantaneously vary their shapes and morphologies is a basic condition for endocytosis, exocytosis and signal transmission, etc.[4−6] The morphology of plasma membranes is the direct sign of cell status; for example, the rupture or partial swallowing of a plasma membrane is the significant evidence for apoptosis induced by drugs.[8−11] In addition, as the first protective barriers of cells, plasma membranes will take actions once they sense injuries from external poison substances (e.g., heavy metal ions).[7] Thus, real time video tracking the plasma membrane is valuable for cell biology, pharmacology, toxicology, and so on. There have been reports on membrane observation by using bright-field microscopy. However, these results lack detailed information due to the low resolution and the color mode. Fluorescence microscopy is a more powerful and reliable method, supplying visual and vivid information. However, this technique shows high dependence on the performances of fluorescent probes.

To date, long time video imaging of the dynamic process of plasma membranes is still a challenge, because common fluorescent membrane markers cannot meet all the requirements, such as stably inserting into membranes, high photostability, intensive and long wavelength emission, etc. Frequently used membrane markers are from DiI and FM families (as shown in Scheme 1). $DiIC_{18}(3)$, a typical example in the DiI family, is a long-chain carbocyanine dye and a highly lipophilic molecule. Normally, $DiIC_{18}(3)$ diffuses into mem-

Scheme 1. Structures of $DiIC_{18}(3)$, FM 4-64 and Mem-SQAC

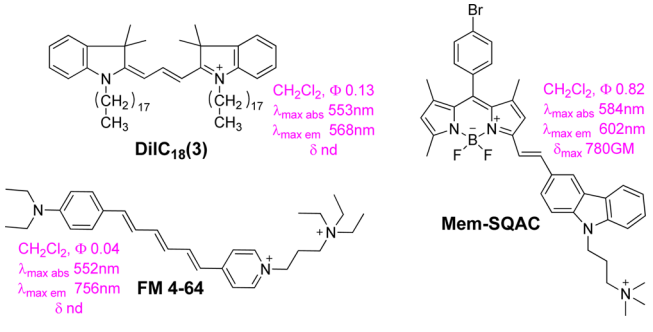

Received: April 12, 2014
Accepted: July 21, 2014
Published: July 21, 2014

Scheme 2. Synthetic Procedures for Mem-SQAC

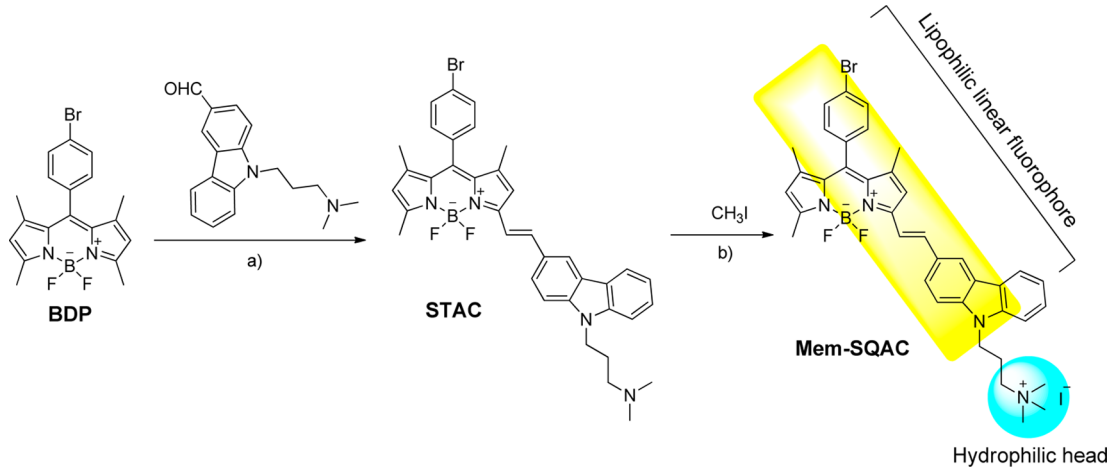

Reaction Condition: (a) piperidine, acetic acid in toluene, reflux by using a Dean−Stark trap, 8h, yield 33%. (b) Methyl iodide in CH_2Cl_2, RT, 10 h, yield 90%.

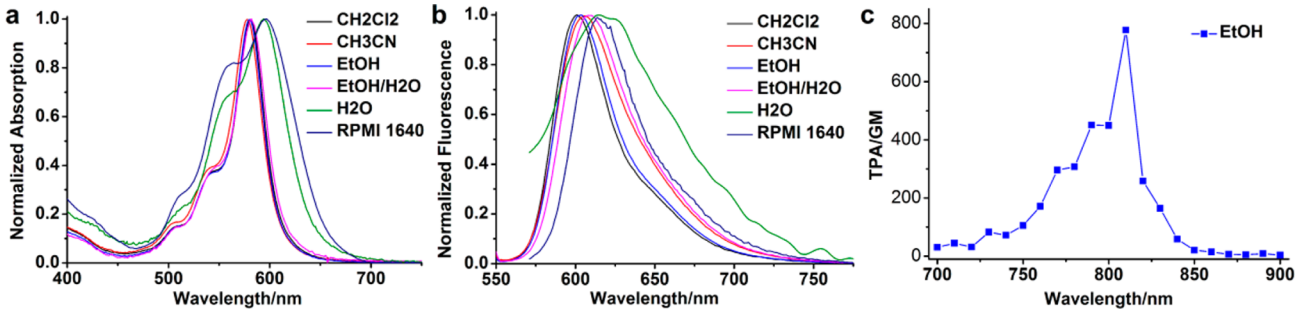

Figure 1. (a) Normalized absorption spectra and (b) normalized fluorescence spectra of Mem-SQAC in different solvents. (c) Two-photon absorption spectra of Mem-SQAC in EtOH.

brane quickly and tends to uniformly label entire cells via lateral diffusion in few minutes.[12,13] Thus, DiIs are preferred to be used for tracing nerve cells[14,15] rather than to dynamically track plasma membranes. In contrast, the FM family, taking FM 4-64 as an example, can bind rapidly and stably to plasma membranes. Their membrane retention is improved due to the polar head in one end of the long and linear molecules. Unfortunately, FMs' poor photostability, possibly due to the unstable polyenoic srtucture, decides that they are not suitable for long time dynamic tracking under strong laser excitation conditions of a confocal microcopy. Besides, when used in multicolor imaging their large fwhm (full width at half-maximum) of spectrum makes it hard to avoid spectrum overlay.[16] Although a few other membrane markers have been reported recently, they are one-photon emitters with relatively short wavelength emissions and their applications in video imaging are rarely demonstrated.[17,18] Therefore, it is still an essential and pressing work to search for markers with good retentiveness within plasma membranes and satisfactory photophysical characteristics, including high photostability and two-photon excitation fluorescence activity.

In this work, a bipolar membrane marker, Mem-SQAC, is developed based on our newly developed long wavelength BODIPY scaffold.[19,20] This membrane marker binds rapidly and stably to the plasma membranes with remarkable fluorescence enhancement and a retention time of more than 30 min in plasma membranes of MCF-7, RAW 264.7, and Hela cells. It also shows excellent optical properties including large extinction coefficients, high fluorescence quantum yields in deep red region, reasonable two-photon absorption cross section, and good photostability. Details of plasma membranes' actions have been exhibited vividly by employing Mem-SQAC during different physiological or toxicological processes, such as heavy metal poisoning and drug induced apoptosis. Particularly, in dynamically tracking the complete endocytosis processes, interesting differences in RAW 264.7 macrophage cells' responses toward two different bacteria have been discovered.

RESULTS AND DISCUSSION

Design and Synthesis of Mem-SQAC. The key point of this designing is the formation of an amphiphilic and bipolar structure. BODIPY-carbazole fluorophore has a rigid and rod-like skeleton that is highly lipophilic (Scheme 2).[20] Grafting a hydrophilic group (a quaternary ammonium salt moiety) in one end of the lipophilic fluorophore attributes to the bipolarity. Mem-SQAC's large and planar π-conjugation enables it to form aggregates in water via $\pi-\pi$ interaction, which could efficiently quench fluorescence. This is a consice way to eliminate the background fluorescence and thus improve the resolution of the target-specific probes.[17,21,22] More importantly, Mem-SQAC has a tendency to stably localize at the lipid−water interface. The high lipophilicity of the rod-like part makes the molecule willing to insert into the membrane, but the polar head pulls the whole molecule, to stop them from penetrating the plasma membrane. In a word, this design enhances the marker's locating stability in membranes and thus extends the

retention time. In addition, the extended conjugation and reasonable intramolecular charge transfer characteristics of Mem-SQAC endows this membrane marker strong deep red emission by two-photon excitation and high photostability, thus solving the photobleaching problem that the other membrane markers have been suffering.

Fundamental Optical Properties and Photostability. Mem-SQAC exhibits satisfactory photophysical properties as a membrane marker. In organic solvents, Mem-SQAC shows typical BODIPYs' properties, such as a high molar extinction coefficient (~111 900 M^{-1} cm^{-1}), small fwhm (full width at half-maximum) of spectrum (~35 nm), high quantum yield (~0.82 in CH_2Cl_2, acetonitrile and EtOH), and also environmental factor-independent (except for in pure water).[19,20] This will promise a homogeneous and stable staining of plasma membranes independent of lipid composition, fraction of the liquid ordered phase, and hydration. Further, two-photon absorption (2PA) spectra have been measured through a femtosecond two-photon-excited fluorescence (TPEF) technique, as shown Figure 1c and Table 1.[23] Mem-SQAC exhibits

Table 1. Photophysical Properties of Mem-SQAC

solvent	λ_{abs} (nm)	λ_{em} (nm)	ε (M^{-1} cm^{-1})	Φ_f[a]	δ[b] (GM)
CH_2Cl_2	584	602	102300	0.82	nd
CH_3CN	580	610	105300	0.80	nd
EtOH	582	606	111900	0.81	780
EtOH/H_2O[c]	582	608	98300	0.72	nd
H_2O	594	615	44200	0.01	nd
H_2O/CTAB[d]	589	617	89900	0.33	nd
RPMI 1640[e]	595	615	60900	0.08	nd

[a]Rhodamine B (Φ_f = 0.69, in MeOH) is used as the standard. [b]Maximum δ at 810 nm in EtOH. [c]EtOH/H_2O = 1/1. [d]CTAB (hexadecyltrimethylammonium bromide) concentration is 20 mM in water. [e]RPMI 1640 with FBS.

reasonable 2PA cross section across the 700−900 nm spectral window with a maximum δ 780 GM at 810 nm. As is known, two-photon microscopy has gained increasingly popularity in biological imaging because of its considerable imaging depth inside intact tissues (>500 μm), inherent three-dimensional resolution without out-of-focus fluorescence, and the limited photobleaching and photodamage to the focal volume. The combination of two-photon excitation and long wavelength emission will be very advantageous over those common used one-photon membrane markers. Employing Mem-SQAC, a bright and high-resolution two-photon fluorescence image of MCF-7 cells is obtained, as shown in Figure S1 (Supporting Information). In the two-photon image, the distributions of fluorescence signal are almost identical with those in the corresponding one-photon image, reflecting the effective emission of **Mem-SQAC** under two-photon excitation conditions. However, two-photon has the advantage of deep penetration with low photodamage and autofluorescence for the fluorescence imaging of tissue or living animals. At the cell level, imaging depth will not be a problem. Thus, we employed all the imaging experiments by using one-photon fluorescence microscopy.

In water, Mem-SQAC readily undergoes aggregation due to its amphiphilicity, which results in drastic changes in the optical properties. The main peak of the absorption bathochromically shifts from 580 nm in organic solvents to 594 nm in water accompanied by a decreasing of the extinction coefficient to 44 200 M^{-1} cm^{-1}. The fwhm is also broadened from 40 to 78 nm, which is the result of the formation of aggregates (Table 1). A Dynamic light scattering (DLS) test is employed to examine the size of the aggregation. It turns out that the dye will form aggregation with an average radius 68 nm (Figure S2, Supporting Information). Furthermore, the critical aggregation concentration (CAC) is determined as 0.40 μM in water by employing ultraviolet spectroscopy (Figure S3, Supporting Information). Corresponding to the change of absorption, the fluorescence is almost completely quenched in water with a quantum yield of 0.01. However, these aggregates could easily be broken up with surfactant in water. After titration with varying amount of CTAB (hexadecyltrimethylammonium bromide), the absorption and fluorescence spectra recover to what they are like in organic solvents (Figure S4a,b, Supporting Information). The final spectra shows a typical monomeric Mem-SQAC characteristic, with a quantum yield of up to 0.33 and an extinction coefficient of up to 89 900 M^{-1} cm^{-1}. These sharp dispersity differences between in water and organic solutions provide an ideal way to increase the signal-to-noise ratio of the target-specific probe, because, in contrast to the intensively fluorescent lipophilic areas, the almost nonfluorescent aqueous surrounding means extremely low background noise.[17,21,22]

Superiorities of Mem-SQAC in Membrane Retention and Photostability: Comparisons with Commercial Membrane Probes. One advantage of Mem-SQAC over commercial membrane probes is its stable localization in plasma membranes. After the the plasma membrane of the cells was washed three times with phosphate buffered saline (PBS), MCF-7, they were stained by Mem-SQAC to maintain the strong fluorescence (Figure 2a,b), whereas membranes stained

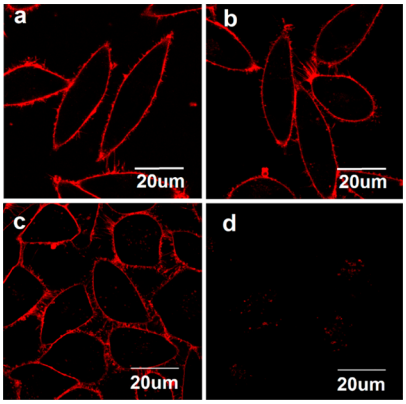

Figure 2. MCF-7 cells stained with 1 μM Mem-SQAC (5 min at 37 °C 5% CO_2) in RPMI 1640 medium without washing (a) and after washing for three times (b) with PBS (λ_{ex} = 559 nm, λ_{em} = 570−630 nm, pseudored color). MCF-7 cells stained with 1 μM FM4-64 (5 min at 37 °C 5% CO2) in RPMI 1640 medium without washing (c) and after washing for three times (d) with PBS (λ_{ex} = 559 nm, λ_{em} = 655−755 nm, pseudored color).

by FM4-64 lose the fluorescence totally (Figure 2c,d). It is clear that FM4-64's retention is not as stable as Mem-SQAC, and so, this commercial probe is easily washed off from the plasma membranes. That is to say, in the application of FM4-64, Do-Not-Wash will be a must. However, without a washing procedure, the continuous exposure of FM4-64 in culture medium will possibly cause the unwanted staining of membrane structures added into the culture in the latter steps. For

example, if we plan to monitor the plasma membranes of macrophage cells during the processes in which they gobble up bacteria (as we will do in the rest of this paper), FM4-64 will not be a good choice, as FM4-64 will not only stain macrophage membranes at first but also the residuary dye will stain bacteria membranes. So, FM4-64 is usable for imaging the static morphology of plasma membranes, but is obviously unfit for long time tracking or costudying with other objects. As for another commercial membrane marker, $DiIC_{18}(3)$, the fluorescence image experiments prove the infeasibility of employing this dye to stain plasma membranes. As shown in Figure S5 (Supporting Information), MCF-7 cells stained by $DiIC_{18}(3)$ exhibit a clear fluorescent pattern involving all intracellular membranes structures. Thus, $DiIC_{18}(3)$ is actually not a specific marker for plasma membranes, not to mention the stable retention.

There have been some interesting reports by Cho et al. and Klymchenko et al. on differentiating the rigid and fluid domains in plasma membrane. Cho et al. developed a TP turn-on probe for the lipid rafts, which allows direct visualization of the lipid rafts in the live cells.[24] Klymchenko et al. designed a Nile Red based probe for monitoring cholesterol and lipid order selectively at the outer leaflet of cell membranes.[27] By contrast, Mem-SQAC's locating ability and emission is independent of lipid order or lipid rafts distribution. As shown in Figure S15 (Supporting Information), fluorescence images of MCF-7 cells are the same before and after being treated with methyl-β-cyclodextrin (MβCD). Stable emission in a plasma membrane means Mem-SQAC is fit for tracking the plasma membrane under different physiological conditions, for example, pathological and toxicological conditions.

The other advantage of Mem-SQAC is its high photostability inherited from the BODIPY family, as is confirmed by two groups of tests. First, photodecompositions of Mem-SQAC's and FM4-64 are conducted by using fluorescence spectrophotometry. After 25 min of irradiation by 560 nm excitation light from a 150 W xenon lamp, FM4-64 is almost totally bleached, but the fluorescence intensity of Mem-SQAC remains as high as 70% (Figure S6b, Supporting Information). This comparison reveals that Mem-SQAC's photostability is much better than that of FM4-64. Second, Mem-SQAC has been compared with other popular fluorophores, including fluorescein, RhB, and BDP.[20] Mem-SQAC shows good photostability, similar to that of BDP, but superior to those of RhB and fluorescein (Figure S6a, Supporting Information). After irradiation by a 500 W iodine−tungsten lamp for 475 min, the fluorescence of Mem-SQAC and that of BDP are maintained as high as 95% and 93% of their initial intensities, respectively, whereas RhB and fluorescein lost 24% and 61%, respectively.

Because the stable localizing and the long times of enduring intensive light irradiation under microcopy are two fundamental requirements for a fluorescent tracker, obviously, Mem-SQAC, outperforming FM4-64 and $DiIC_{18}(3)$ in above two aspects, is more suited to video image the dynamic changes of plasma membranes of live cells.

Cellular Uptake Studies. In cellular uptake studies, it is found that Mem-SQAC can quickly stain plasma membranes of different cell lines. Three cell lines including human breast carcinoma (MCF-7), helacyton gartleri (Hela) and macrophage cells (RAW 264.7) are used for imaging studies. All these cell lines could be stained within 5 min and show clear and bright fluorescence images of plasma membrane. The fluorescent images show a high signal-to-noise ratio, even without washing the stained cells. MCF-7 cells are incubated with 1 μM Mem-SQAC solution in RPMI 1640 medium and imaged after 5 min without washing. Fluorescence images of MCF-7 are given in Figure 2a as representative.

In contract to its rapid staining of plasma membranes, Mem-SQAC stays longer than 30 min in plasma membranes (see Figures S7−9, Supporting Information) before its slowly passes through the membranes. During that period, the fluorescence images of the plasma membranes remain very clear. After 30 min, the fluorescence signal inside the cells begins to appear and increases gradually, whereas that of the plasma membranes decreases. After 60 min, pronounced intracellular accumulation of Mem-SQAC is observed in some small vesicular organelles (Figures S7−9, Supporting Information). Mem-SQAC does not diffuse into cells as quickly as it is incorporated into plasma, which indicates that the dye prefers to stay inside the plasma membranes. The slow entering into a cell indicates that uptake of Mem-SQAC may be via endocytosis other than passive diffusion, which is confirmed by the following studies on endocytosis inhibition and colocalization imaging. When endocytosis is inhibited by lowering the incubating temperature from 37 to 4 °C, it is found that the uptake of Mem-SQAC is dramatically slowed (Figures S7−9, Supporting Information). It is well-known that lysosomes are the destinations of endocytosis. But there are also other major types of membrane-composed subcellular organelles, such as mitochondria and endoplasmic reticulums. To this end, three fluorescence imaging experiments using Mem-SQAC and standard lysotracker, mitotracker, or ERtracker to costain cells have been performed. The good colocalization result is obtained only in the case of lysotraker, which proves that the small vesicular organelles where Mem-SQAC accumulates are lysosomes (Figures S10−12, Supporting Information).[25,26]

Given that plasma membranes of cells are rebuilt consistently and rapidly during metabolism, 30 min of retention for a small molecular tracker is hardly achievable, and thus, Mem-SQAC is commendable. In our later studies, such a retention time proves to be sufficient for tracking some biological processes involving plasma membranes.

Monitoring Morphology Variation of Plasma Membrane under Physiological or Toxicological Conditions. Apoptosis is one of the widely studied biological processes. There have been some reports on the studies of plasma membranes' changes during apoptosis.[29,30] Environment-sensitive fluorescent probes have been employed to detect change in the microenvironments in plasma membranes. However, these results indicate only the final status of plasma membranes of apoptosis cells. They did not give complete dynamic records of the process of cell apoptosis induced by drugs. Tracking this process needs a long retention time of the probe in plasma membranes as apoptosis is a relatively slow process.

Mercury is one of the most toxic heavy metal elements that leads to the malfunction of cells. Thus, there is an intensive reported on the tool, fluorescence probes, for the detecting of intracellular Hg^{2+}.[27,28] However, there is hardly any report on visually exhibiting the immediate responses of cells against such a poisoning substance. For example, it is not clarified how and how fast the morphology of plasma membranes will change upon exposure to Hg^{2+}.

We try to illustrate the potential of Mem-SQAC contributing to the above two important research areas. In our studies, real time membrane tracking exhibits detailed membrane move-

ment intuitively and vividly during apoptosis and heavy metal poisoning.

In the first study, apoptosis is induced by incubating stained cells with 10 μM dexamethasone (an anti-inflammatory and immunosuppressant clinical drug that could induce cell apoptosis) for 40 min. Due to Mem-SQAC's affinity to the membrane and high fluorescence intensity, the complete apoptosis process of the same cells is recorded by using a confocal microscope. During this process, plasma membranes gradually become irregular and waved, although cell contours roughly maintain their initial shapes (Figure S13, Supporting Information).[8] Figure 3a shows the overlay of plasma membranes in final status (pseudogreen color) and original status (pseudored color). The picture accurately demonstrates the morphology change of single cell before and after apoptosis in detail.

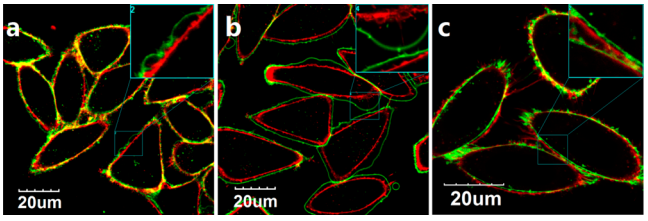

Figure 3. (a) Overlay fluorescence image of stained MCF-7 cells before (pseudored color) and after (pseudogreen color) being incubated with dexamethasone (final concentration 10 μM) for 40 min. (λ_{ex} = 559 nm, λ_{em} = 570−630 nm). (b) Overlay fluorescence image of stained MCF-7 cells (staining for 5 min and washing twice with PBS) before (pseudored color) and after (pseudogreen color) being incubated with Hg^{2+} (final concentration 100 μM) for 40 min. (c) Overlay fluorescence image of stained MCF-7 cells (staining for 5 min and washing twice with PBS) at 0 and 40 min.

In contrast to drug induced apoptosis, contact with Hg^{2+} results in more pronounced changes in cell contours. (Figure 3b). Sequential image results are listed in Figure S14 (Supporting Information). Generally speaking, the whole plasma membranes become swollen evidently, while they look still smooth but neither ruptured nor irregular. Cells just keep on being filled up by extracellular water. It is a passive result due to membrane function loss, which is different from apoptosis. Apoptosis is a programed result of many biological actions and usually this process is accompanied by plasma membranes' being irregular and even being broken up.

Compared with unstimulated cells (Figure 3c), the sharply different tendencies of morphological changes monitored by employing Mem-SQAC can be the potential indicators for different injuries induced by external chemical species, which confirms that Mem-SQAC is an applicable probe in the fields of toxicology and pharmacology.

Tracking Endocytosis Stimulated by Bacterium. Endocytosis is an important process during the metabolism of cells based on the mobility of plasma membranes. Tracking the movement of plasma membranes will help to more deeply understand this process. There are some former studies about the endocytosis of macrophages toward bacteria by using fluorescence microscopy or scanning electron microscopy (SEM). Although SEM could provide images with high resolution, it is not fit for living cells imaging.[31] Most reported results by fluorescence microscopy are static images of the final status after the endocytosis is finished. This research did not pay much attention to the role that plasma membranes play in corresponding processes.[32,33] There is a scarce dynamic record of the endocytosis of unstained macrophages toward green bacteria.[31] The reports illustrated the movement of macrophages during the endocytosis in bright-field microscopy. However, they could not give a direct illustration for the transfer of plasma membranes.

We successfully video image the full endocytosis of macrophages and MCF-7 cells, respectively, by using Mem-SQAC to continuously track plasma membranes. To our knowledge, we observed some interesting phenomena that have not been available in literature previously. RAW 264.7 is typical phagocyte, whose plasma membranes show high activity, especially when it is stimulated by the environment. To this end, RAW 264.7 cells are stained in advance, and then incubated with *Staphyloccocus aureus* (GFP expressed). The process in which macrophages swallow the ball shaped bacteria is recorded by confocal fluorescence microscopy (Figure 4 and video1, see the Supporting Information). Irregular membrane protrusions take place where the *S. aureus* is getting close. The dynamic fluorescent pictures show that evident ruffles (blue

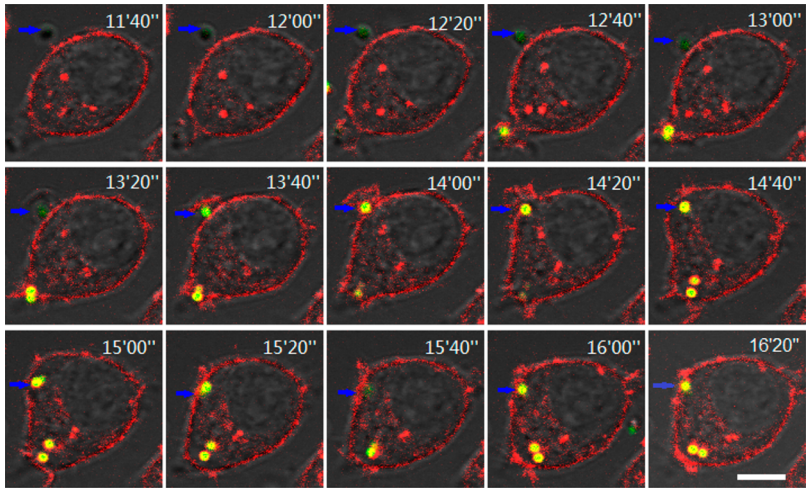

Figure 4. Dynamic fluorescent pictures of RAW 264.7 cell swallowing *S. aureus* (GFP expressed). For Mem-SQAC (λ_{ex} = 559 nm, λ_{em} = 570−630 nm, pseudored color) and for GFP (λ_{ex} = 488 nm, λ_{em} = 500−560 nm, pseudogreen color). The scale bar is 10 μM.

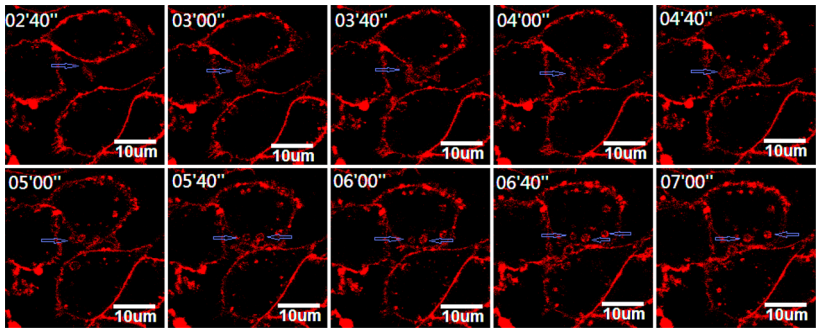

Figure 5. Dynamic fluorescent pictures of the formation of vesicles in RAW 264.7. (λ_{ex} = 559 nm, λ_{em} = 570−630 nm, pseudored color).

arrow) at the surface of plasma membranes stretch toward the *S. aureus* and then it is incorporated into the cell. After the *S. aureus* is completely uptaken, the ruffles "calm down", and the active surface becomes smooth once again. During this process, Mem-SQAC stays stable in the active plasma membranes and exhibits the detailed movement of the membrane. We could also see that the green bacteria turn yellow after they are swallowed into cells (fluorescence intensity correlation, see Figure S16 (Supporting Information). The yellow is the overlay of green bacteria and the red membrane structure, the phagocytotic vesicle. This phenomenon demonstrates detailed information on plasma membranes' packing of bacteria when the uptake happens.

However, when the same experiment is conducted by using *Escherichia coli*, a different phenomenon is observed. Fluorescent vacuoles in big size (~2 μm) are observed when stained Macrophages are used to swallow *E. coli* (Figure 5 and video2, see the Supporting Information). These vacuoles take place in plasma membranes soon after *E. coli* is added. First, the plasma membranes become very active, and then big ruffles take place. As these ruffles stretch out and return, big vacuoles form and enter into the cell. These vacuoles stay stable in the cell for quite a long time. Mem-SQAC stays stable in the active membrane and moves within the vesicle into the cells. Even though the uptake of *E. coli* is hard to observe, macrophages become very active under the stimulation of *E. coli*. Different from *S. aureus*, *E. coli* is a Gram-negative, facultative anaerobic, rod-shaped bacterium with its cell wall containing lipopolysaccharide (LPS). LPS is a toxin that may activate macrophages and stimulate cells to generate reactive oxygen species.[34] To the best of our knowledge, there is no report on dynamically visualizing the details of two bacterium endocytosis by macrophages cells. In the previous endocytosis studies under fluorescence microscopy, usually, it is the fluorescent beads or polymeric particles but not the bacteria that are used as objects to be swallowed, the plasma membranes are not fluorescently labeled, and most of these reports have not provided any dynamic videos.[3,9]

As for the experiment on swallowing Staphyloccocus aureus by MCF-7, plasma membranes of these cells do not show active uptake of bacteria as macrophages (video3, see the Supporting Information). Stained MCF-7 cells hardly show any morphology change. There does not appear to be clear ruffles or a big vesicle. To be exact, the cells are passively invaded by these bacteria. The bacteria attack the plasma membranes and sunk parts form as the bacteria enter into the cells. Still, the "swallowed" bacteria are packed in the red fluorescent vesicle. These results demonstrate the potential of Mem-SQAC as a membrane marker to visualize detailed dynamic processes of plasma membranes.

Cytotoxicity Study. The cytotoxicity of Mem-SQAC is low. MTT assay (Figure S17, Supporting Information) has revealed that even through incubation with a much higher concentration (5 μM) than the optimized level, ~90% of MCF-7 and ~80% of macrophage cells survive after 24 h. That is to say, it is safe to employ the long time tracking experiment under the optimized concentration (~1 μM). This is a favorable characteristic of a practical membrane marker applied in living cells.

CONCLUSION

In summary, we develop a new membrane marker, Mem-SQAC, which exhibits a long retention time over 30 min in plasma membranes of MCF-7, RAW 264.7, and Hela cells. It can bind rapidly and stably to the plasma membranes due to the reasonable bipolarity balance caused by the cooperation of the rod-like lipophilic BODIPY chromophore at one end of the molecule and a highly hydrophilic quaternary ammonium at the other end. Its drastic differences in the optical properties between water (nonfluorescent) and lipophilic (strongly fluorescent) environment make it an idea candidate for membrane tracking. In addition, the red fluorescent Mem-SQAC has the advantages of high photostability and a large two-photon absorption cross section.

A series of experiments to track plasma membranes during different physiological or toxicological processes confirm Mem-SQAC's applicability in cell research. Distinct differences of plasma membrane morphology changes are found during tracking target cells that undergo drug induced apoptosis and Hg^{2+} invading. These studies demonstrate Mem-SQAC's potential application in pharmacology and toxicology research. In the endocytosis experiment of RAW 264.7 cells toward different types of bacteria, different actions of RAW264.7 cells are also exhibited. For example, in the presence of *S. aureus*, RAW 264.7 plasma membranes stretch tentacles outward and swallow single bacteria efficiently, whereas stimulation by *E. coli* activates RAW 264.7 to concave the plasma membranes inward and form big size (~2 μm) fluorescent vacuoles without inclusion of a bacterium. To our knowledge, these results have not been available previously, which is proof of Mem-SQAC's applicability in cell research.

EXPERIMENTAL SECTION

Materials. Carbazole aldehydes and DC-BDP are synthesized according to standard procedures.[20] Toluene is dried over suitable reagents and distilled under argon immediately prior to use. The commercial dyes DND-189 and Rh-123 are used as received with a

purity >99% (checked by spectroscopic and chromatographic methods). Solvents for spectra studies are of spectroscopic grade and are used without purification.

General Methods. The 400 (^{1}H) MHz NMR and 100 (^{13}C) MHz NMR spectra are registered at room temperature using perdeuterated solvents as the internal standard. Melting points were obtained with a capillary melting point apparatus in open-ended capillaries and are uncorrected. Chromatographic purification is conducted with silica gel. All solvent mixtures are given as volume/volume ratios. The slit width is 3 nm for both excitation and emission during fluorescence spectra recording. Relative quantum efficiencies of fluorescence of compounds are obtained by comparing the areas under the corrected emission spectrum of the test sample in diluted solvents with that of Rhodamine B (Φ_F = 0.69) in methanol. Nondegassed, spectroscopic grade toluene and a 10 mm quartz cuvette are used. Dilute solutions (0.02 < A < 0.08) are used to minimize reabsorption effects. Quantum yields are determined using eq 1:

$$\Phi_F^{(\text{sample})} = \Phi^{(\text{standard})} \times (\text{Abs}^{(\text{standard})} \times F^{(\text{sample})}) / (\text{Abs}^{(\text{sample})} \times F^{(\text{standard})}) \quad (1)$$

Where $\Phi^{(\text{standard})}$ is the reported quantum yield of the standard, Abs is the absorbance at the excitation wavelength, and F is the integrated emission spectra.

Effects on Cell Growth/Viability. All cell lines are maintained under standard culture conditions (atmosphere of 5% CO_2 and 95% air at 37 °C) in RPMI 1640 medium, supplemented with 10% fetal bovine serum (FBS). The cytotoxic effect of Mem-SQAC is assessed using the MTT assay. Briefly, the cells in the exponential phase of growth are used in the experimentation. 1.5×10^3 cells/well are seeded onto 96-well plates and allowed to grow for 24 h prior to treatment with Mem-SQAC. The incubation time of Mem-SQAC is 5 min. At the end of this time, the Mem-SQAC containing medium is replaced with PBS, and MTT is then added to each well (final concentration = 0.5 mg/mL) for 4 h at 37 °C and formazan crystals formed through MTT metabolism by viable cells are dissolved in dimethyl sulfoxide (DMSO). Optical densities are measured at 570 nm.

Culture of Cell Lines and Fluorescent Imaging. All cell lines are maintained under standard culture conditions (atmosphere of 5% CO_2 and 95% air at 37 °C) in RPMI 1640 medium, supplemented with 10% FBS. Growth of MCF-7, RAW 264.7, and Hela cells in the exponential phase of growth on 35 mm glass-bottom culture dishes (Φ 20 mm) was conducted for 1−2 days to reach 70−90% confluence. These cells are used in colocalization experimentation. The cells are washed three times with RPMI 1640, and then are incubated with 2 mL containing Mem-SQAC (1 μM) and Rh-123 (1 μM) or DND189 (1 μM) in an atmosphere of 5% CO_2 and 95% air at 37 °C. For cells incubated at 4 °C, ice is used. Mem-SQAC is first prepared as a DMSO solution with a concentration of 1 mM, and is diluted with RPMI 1640 for cells incubating. Cells are washed twice with 1 mL PBS at room temperature, and 1 mL RPMI 1640 culture medium is added and then the solution is observed under a confocal microscope (Olympus FV1000).

Photostability. Men-SQAC, BDP, RhB, and fluorescein are dissolved in solution at a concentration of 10.0 μM, respectively. The solutions are irradiated under a 500 W iodine−tungsten lamp for 7 h at a distance of 250 mm away. An aqueous solution of sodium nitrite (50.0 g/L) is placed between the samples and the lamp as a light filter (to cut off the light shorter than 400 nm) and heat filter. The photostabilities are expressed in terms of remaining fluorescence (%) calculated from the changes of fluorescence at the fluorescence maximum before and after irradiation by the iodine−tungsten lamp. Comparison between Mem-SQAC and FM4-64 is employed by using a fluorescence spectrophotometer. Two probes are dissolved in chloroform at a concentration of 10.0 μM and irradiated by 560 nm excitation light from a 150 W xenon lamp. The photostabilities are expressed in the terms of remaining fluorescence (%) calculated from the changes of fluorescence at the fluorescence maximum before and after irradiation by a xenon lamp.

Synthesis of Mem-SQAC. *STAC.* BDP (1.11 mmol, 500 mg) and *N*−*N*′,*N*′-dimethylpropyl-4-carbazole aldehyde (1.11 mmol, 310 mg) were added to a 100 mL round bottomed flask containing 50 mL of toluene and to this solution is added piperidine (1 mL) and acetic acid (1 mL). The mixture is heated under reflux by using a Dean−Stark trap, and the reaction is monitored by TLC 30:1 (v/v) CH_2Cl_2:CH_3OH (R_f = 0.3). When all the starting material has been consumed, the mixture is cooled to room temperature and solvent is evaporated. Water (300 mL) is added to the residue, and the product is extracted into the CH_2Cl_2 (3 × 200 mL). The organic phase is dried over Mg_2SO_4 and evaporated, and the residue is purified by Al_2O_3 column chromatography using 30:1 CH_2Cl_2:CH_3OH as the eluent, which yielded the desired product STAC as purple powder (243 mg, 33%). mp: 243−245 °C. ^{1}H NMR ($CDCl_3$, 400 MHz): δ 8.28 (1H, s), 8.17 (1H, d), 7.64−7.79 (4H, m), 7.21−7.26 (5H, t), 6.68 (1H, s), 6.01 (1H, s), 4.40−4,42 (2H, t), 2.63 (3H, s), 2.25−2.31 (8H, m), 2.03−2.06 (2H, t), 1.43−1.49 (6H, d), 1.27 (1H, s). ^{13}C NMR ($CDCl_3$, 100 Hz): δ 154.5, 142.7, 141.5, 141.2, 138.9, 134.5, 132.5, 130.5, 127.9, 126.3, 125.8, 123.6, 123.4, 123.2, 121.2, 120.8, 120.6, 119.7, 118.2, 116.4, 109.4, 109.3, 56.7, 45.6, 41.0, 27.1, 15.2, 14.9, 14.8. m/z (TOF MS ES): Calcd $[M + H]^+$ for $C_{37}H_{37}BBrF_2N_4$: 665.2184. Found: 665.2271.

Mem-SQAC. STAC (0.15 mmol, 100 mg) is dissolved in 5 mL of CH_2Cl_2, and methyl iodide (0.2 mL) is added. The solution is stirred at room temperature for 10 h. The solvent is evaporated, and the residue is recrystallized by *n*-hexane (109 mg, 90%). mp: 211−214 °C. ^{1}H NMR (DMSO, 400 MHz): δ 8.28−8.40 (1H, d), 7.78 (3H, t), 7.30−7.54 (2H, t), 7.02 (1H, s), 6.21 (1H, s), 4.51 (1H, s), 3.46 (1H, s), 3.04 (3H, s), 2.25 (2H, s), 1.41−1.47 (3H, d), 1.23 (2H, s), 0.853 (1H, s). m/z (TOF MS ES): Calcd M^+ for $C_{38}H_{39}BBrF_2N_4$: 679.2414. Found: 679.2431.

■ ASSOCIATED CONTENT

Ⓢ Supporting Information

Additional spectrum, fluorescence imaging, and ^{1}H and ^{13}C spectra. This material is available free of charge via the Internet at http://pubs.acs.org.

■ AUTHOR INFORMATION

Corresponding Author

*Y. Xiao. E-mail: xiaoyi@dlut.edu.cn.

Notes

The authors declare no competing financial interest.

■ ACKNOWLEDGMENTS

Y. Xiao thanks National Natural Science Foundation of China (Nos. 21174022, 21376038), National Basic Research Program of China (No. 2013CB733702) and Specialized Research Fund for the Doctoral Program of Higher Education (No. 20110041110009) for financial support.

■ REFERENCES

(1) Schlessinger, J.; Axelrod, D.; Koppel, D.; Webb, W.; Elson, E. Lateral Transport of a Lipid Probe and Labeled Proteins on a Cell Membrane. *Science* **1977**, *195*, 307−309.

(2) Grimmer, S.; Deurs, B.; Sandvig, K. Membrane Ruffling and Macropinocytosis in A431 Cells Require Cholesterol. *J. Cell Sci.* **2002**, *115*, 2953−2962.

(3) Rejman, J.; Oberle, V.; Zuhorn, I.; Hoekstra, D. Size-Dependent Internalization of Particles via the Pathways of Clathrin-and Caveolae-mediated Endocytosis. *Biochem. J.* **2004**, *377*, 159−169.

(4) Koivusalo, M.; Welch, C.; Hayashi, H.; Scott, C. C.; Kim, M.; Alexander, T.; Touret, N.; Hahn, K. M.; Grinstein, S. Amiloride Inhibits Macropinocytosis by Lowering Submembranous pH and Preventing Rac1 and Cdc42 signaling. *J. Cell Biol.* **2010**, *188*, 547−563.

(5) Kahya, N.; Scherfeld, D.; Bacia, K.; Poolman, B.; Schwille, P. Probing Lipid Mobility of Raft-exhibiting Model Membranes by

Fluorescence Correlation Spectroscopy. *J. Biol. Chem.* **2003**, *278*, 28109−28115.
(6) Brown, D. A.; London, E. Functions of Lipid Rafts in Biological Membranes. *Annu. Rev. Cell Dev. Biol.* **1998**, *14*, 111−136.
(7) Wyllie, A. H. Glucocorticoid-induced Thymocyte Apoptosisis Associated with Endogenous Endonuclease Activation. *Nature* **1980**, *284*, 555−556.
(8) Zwaal, R. F.; Schroit, A. J. Pathophysiologic Implications of Membrane Phospholipid Asymmetry in Blood Cells. *Blood* **1997**, *89*, 1121−1132.
(9) Fadeel, B.; Xue, D. The Ins and Outs of Phospholipid Asymmetry in the Plasma Membrane: Roles in Health and Disease. *Crit. Rev. Biochem. Mol. Biol.* **2009**, *44*, 264−277.
(10) Gutknecht, J. Inorganic Mercury (Hg^{2+}) Transport through Lipid Bilayer Membranes. *J. Membr. Biol.* **1981**, *61*, 61−66.
(11) Hinz, B.; Hirschelmann, R. Dexamethasone Megadoses Stabilize Rat Liver Lysosomal Membranes by Non-Genomic and Genomic Effects. *Pharm. Res.* **2000**, *17*, 1489−1493.
(12) Honig, M. G.; Hume, R. I. DiI and DiO: Versatile Fluorescent Dyes for Neuronal Labeling and Pathway Tracing. *Trends Neurosci.* **1989**, *12*, 333−341.
(13) Struck, D. K.; Pagano, R. E. Insertion of Fluorescent Phospholipids into the Plasma Membrane of a Mammalian Cell. *J. Biol. Chem.* **1980**, *255*, 5404−5410.
(14) Ragnarson, B.; Bengtsson, L.; Haegerstrand, A. Labeling with Fluorescent Carbocyanine Dyes of Cultured Endothelial and Smooth Muscle Cells by Growth in Dye-containing Medium. *Histochemistry* **1992**, *97*, 329−333.
(15) Li, N.; Yang, H.; Lu, L.; Duan, C.; Zhao, C.; Zhao, H. Comparison of the Labeling Efficiency of Brdu, DiI and Fish Labeling Techniques in Bone Marrow Stromal Cells. *Brain Res.* **2008**, *1215*, 11−19.
(16) Rea, R.; Li, J.; Dharia, A.; Levitan, E. S.; Sterling, P.; Kramer, R. H. Streamlined Synaptic Vesicle Cycle in Cone Photoreceptor Terminals. *Neuron* **2004**, *41*, 755−766.
(17) Heek, T.; Nikolaus, J.; Schwarzer, R.; Fasting, C.; Welker, P.; Licha, K.; Herrmann, A.; Haag, R. An Amphiphilic Perylene Imido Diester for Selective Cellular Imaging. *Bioconjugate Chem.* **2013**, *24*, 153−158.
(18) Yan, P.; Xie, A.; Wei, M.; Loew, L. M. Amino (Oligo) Thiophene-based Environmentally Sensitive Biomembrane Chromophores. *J. Org. Chem.* **2008**, *73*, 6587−6594.
(19) Zhang, D.; Martín, V.; García-Moreno, I.; Costela, A.; Pérez-Ojeda, M. E.; Xiao, Y. Development of Excellent Long-Wavelength BODIPY Laser Dyes with a Strategy that Combines Extending π-Conjugation and Tuning ICT Effect. *Phys. Chem. Chem. Phys.* **2011**, *13*, 13026−13033.
(20) Zhang, X.; Xiao, Y.; Qi, J.; Qu, J.; Kim, B.; Yue, X.; Belfield, K. D. Long-Wavelength, Photostable, Two-Photon Excitable BODIPY Fluorophores Readily Modifiable for Molecular Probes. *J. Org. Chem.* **2013**, *78*, 9153−9160.
(21) Ogawa, M.; Kosaka, N.; Choyke, P. L.; Kobayashi, H. H-Type Dimer Formation of Fluorophores: A Mechanism for Activatable in Vivo Optical Molecular Imaging. *ACS Chem. Biol.* **2009**, *4*, 535−546.
(22) Kobayashi, H.; Choyke, P. L. Target-Cancer-Cell-Specific Activatable Fluorescence Imaging Probes: Rational Design and in Vivo Applications. *Acc. Chem. Res.* **2011**, *44*, 83−90.
(23) Xu, C.; Webb, W. W. Measurement of Two-Photon Excitation Cross Sections of Molecular Fluorophores with Data from 690 to 1050 nm. *J. Opt. Soc. Am. B* **1996**, *13*, 481−491.
(24) Kim, H. M.; Jeong, B. H.; Hyon, J. Y.; An, M. J.; Seo, M. S.; Hong, J. H.; Lee, K. J.; Kim, C. H.; Joo, T.; Hong, S. C.; Cho, B. R. Two-Photon Fluorescent Turn-On Probe for Lipid Rafts in Live Cell and Tissue. *J. Am. Chem. Soc.* **2008**, *130*, 4246−4247.
(25) Mellman, I.; Fuchs, R.; Helenius, A. Acidification of the Endocytic and Exocytic Pathways. *Annu. Rev. Biochem.* **1986**, *55*, 663−700.
(26) Ralph, M.; Steinman, I.; Mellman; William, A.; Muller; Zanvil, A. C. Endocytosis and the Recycling of Plasma Membrane. *J. Cell Biol.* **1983**, *96*, 1−27.
(27) Kucherak, O. A.; Oncul, S.; Darwich, Z.; Yushchenko, D. A.; Arntz, Y.; Didier, P.; Mély, Y.; Klymchenko, A. S. Switchable Nile Red-based Probe for Cholesterol and Lipid Order at the Outer Leaflet of Biomembranes. *J. Am. Chem. Soc.* **2010**, *132*, 4907−4916.
(28) Demchenko, A. P.; Mély, Y.; Duportail, G.; Klymchenko, A. S. Monitoring Biophysical Properties of Lipid Membranes by Environment-sensitive Fluorescent Probes. *Biophys. J.* **2009**, *96*, 3461−3470.
(29) Zhang, X.; Xiao, Y.; Qian, X. A Ratiometric Fluorescent Probe Based on FRET for Imaging Hg^{2+} Ions in Living Cells. *Angew. Chem., Int. Ed.* **2008**, *47*, 8025−8029.
(30) Vedamalai, M.; Wu, S. P. A BODIPY-based Colorim Etric and Fluorometric Chemosensor for Hg(II) Ions and its Application to Living Cell Imaging. *Org. Biomol. Chem.* **2012**, *10*, 5410−5416.
(31) Möller, J.; Löhmann, T.; Chabria, M.; Hall, H.; Vogel, V. Macrophages Lift off Surface-bound Bacteria Using a Filopodium-Lamellipodium Hook-and-Shovel Mechanism. *Sci. Rep.* **2013**, *3*, 2884.
(32) Groesdonk, H. V.; Schlottmann, S.; Richter, F.; Georgieff, M.; Senftleben, U. Escherichia Coli Prevents Phagocytosis-induced Death of Macrophages via Classical NF-B Signaling, A Link to T-Cell Activation. *Infect. Immun.* **2006**, *74*, 5989−6000.
(33) Häcker, H.; Fürmann, C.; Wagner, H.; Häcker, G. Caspase-9/-3 Activation and Apoptosis are Induced in Mouse Macrophages upon Ingestion and Digestion of Escherichia Coli Bacteria. *J. Immunol.* **2002**, *169*, 3172−3179.
(34) Yu, H.; Xiao, Y.; Jin, L. A Lysosome-targetable and Two-Photon Fluorescent Probe for Monitoring Endogenous and Exogenous Nitric Oxide in Living Cells. *J. Am. Chem. Soc.* **2012**, *134*, 17486−17489.